

Metastable breathers and local diamagnetism in two-dimensional nonlinear metamaterials

Cite as: Low Temp. Phys. **46**, 712 (2020); <https://doi.org/10.1063/10.0001369>

Submitted: 20 May 2020 . Published Online: 30 July 2020

O. V. Charkina, and M. M. Bogdan



View Online



Export Citation



CrossMark

LOW TEMPERATURE TECHNIQUES
OPTICAL CAVITY PHYSICS
MITIGATING THERMAL
& VIBRATIONAL NOISE

DOWNLOAD THE WHITE PAPER

downloads.montanainstruments.com/optical_cavities

MONTANA INSTRUMENTS
COLD SCIENCE MADE SIMPLE



Metastable breathers and local diamagnetism in two-dimensional nonlinear metamaterials

Cite as: Fiz. Nizk. Temp. **46**, 845–856 (July 2020); doi: [10.1063/10.0001369](https://doi.org/10.1063/10.0001369)

Submitted: 20 May 2020



O. V. Charkina^{1,a)} and M. M. Bogdan^{1,2}

AFFILIATIONS

¹B. Verkin Institute for Low Temperature Physics and Engineering, National Academy of Sciences of Ukraine, 47 Nauki Ave., Kharkiv 61103, Ukraine

²V.N. Karazin Kharkiv National University, 4 Svobody Sq., Kharkiv 610022, Ukraine

^{a)}Author to whom correspondence should be addressed: charkina@ukr.net

ABSTRACT

This article investigates the dynamic properties of two-dimensional nonlinear magnetic metamaterials consisting of nanoscale elements. The authors propose a model for a two-dimensional lattice of capacitively and inductively coupled split rectangular nanoresonators. It has been shown that the long-wave dynamics of this two-dimensional lattice are described by a regularized two-dimensional nonlinear Klein–Gordon equation, which has been solved in the form of two sequences of two-dimensional dynamic solitons on a pedestal of homogeneous forced oscillations, using an asymptotic method and taking into account the action of electromotive force (EMF) induced by an electromagnetic wave. The authors have calculated a diamagnetic response to an electromagnetic field in the terahertz range in the metamaterial region, where a breather is excited and oscillates in antiphase to a homogeneous background. The evolution of long-lived metastable breathers has been numerically studied, and two scenarios – collapse and decay – have been established for the development of their instability depending on the parameters of the induced EMF and inductive coupling between nanoresonators. It has been found that at the boundary between these scenarios, the final result of the transformation of the breathers is the chimera state of the metamaterial with a large-amplitude breather that generates stochastic waves.

Published under license by AIP Publishing. <https://doi.org/10.1063/10.0001369>

INTRODUCTION

In the early 21st century, a remarkable scientific and technological achievement was the experimental implementation of the idea of artificial metamaterials with a negative refractive index for electromagnetic waves in the radio to microwave range.^{1–3} Such metamaterials have unique properties⁴ that can be used to create super lenses unconstrained by the diffraction limit, metamaterial cloaking, electromagnetic sensors, compact antennae, and other devices. At a macroscopic level, two-dimensional metamaterials are structured as a lattice of inductively coupled split-ring resonators, which provide negative magnetic permeability in the corresponding frequency range, while those with a lattice of metal rods, which has a negative dielectric constant, together form a negative refractive index medium.

Various research groups have recently been struggling to develop metamaterials consisting of nanoscale elements in order to get as close as possible to the terahertz and optical range of electromagnetic waves. The development of artificial metamaterials with

nanoscale structural elements and the study of their properties have fostered a new subject area in nanophysics. The nanostructured elements of a magnetic metamaterial that have already been technologically implemented are metal square open loops with characteristic sizes of the order of hundreds of nanometers, for which the resonant frequency of electromagnetic waves is in the terahertz range.⁵

Reducing the sizes of metamaterial elements when approaching the optical range creates difficulties in achieving the required values of both the negative permittivity and magnetic permeability. In nanoscale split resonators, linear magnetic resonance in waves with a length of about a micron is very weak^{6,7} but still capable of providing negative magnetic permeability.

At the same time, the idea has been recently expressed that regions with negative magnetic permeability may manifest with the appearance of nonlinear excitations in one- and two-dimensional magnetic metamaterials.^{8,9} In particular, it has been shown that lattices of inductively coupled split-ring resonators with nonlinear elements (e.g. diodes) can be considered as

nonlinear transmission lines such as two dimensional networks. Numerical simulation has revealed that an alternating magnetic field in them can excite discrete breather-type pulses localized in several resonators and cause their local diamagnetic response. Nonlinear magnetic metamaterials can be implemented in various ways,¹⁰ ranging from incorporating Josephson junctions into split resonators as nonlinear elements¹¹ to creating metamaterials in the form of chains of magnetic molecular clusters (so-called magnetic molecules),^{12,13} or “ferromagnet-superconductor” superlattices.¹⁴

In Ref. 16, in contrast to the analysis of the nonlinear dynamics of metamaterials performed in most studies using numerical calculations,^{9,10,15} we proposed an analytical approach to describing the effect of local negative magnetic permeability in one-dimensional nonlinear magnetic metamaterials. It was shown that the long-wave dynamics and magnetic properties of one-dimensional systems composed of inductively and capacitively coupled split-ring resonators are described by the dispersive regularized nonlinear Klein–Gordon equation.¹⁷ An asymptotic method was used to find dynamic soliton solutions on a “pedestal,” i.e., one-dimensional breathers which are excited by a high-frequency magnetic field and oscillate in antiphase with respect to homogeneous oscillations, thereby resulting in the occurrence of extended

regions with negative magnetic susceptibility and permeability in the nonlinear metamaterial. Augmented by a medium with a negative permittivity, this system forms a “left-handed” metamaterial in which regions with breather excitations are transparent to electromagnetic radiation, which makes it possible to observe them experimentally. Below, it is shown how this analytical approach is generalized to the case of two-dimensional metamaterials with nanostructured elements, for which the development of a local diamagnetic response theory is not only of theoretical, but is also of practical interest, because two-dimensional magnetic metamaterials can serve as coatings with unique properties with respect to electromagnetic waves close to the terahertz and optical ranges.

REGULARIZED NONLINEAR KLEIN-GORDON EQUATIONS FOR A TWO-DIMENSIONAL NONLINEAR METAMATERIAL

Theoretically, a two-dimensional system of split-ring resonators with nonlinear elements was considered in Ref. 9 as an electrical network of inductively interacting LC circuits. For such a two-dimensional system, the discrete equations describing the electromagnetic excitations in a metamaterial have the form

$$\left\{ \begin{array}{l} L \frac{dI_{n,m}}{d\tau} + RI_{n,m} + U_{n,m} - L_x \left(\frac{dI_{n-1,m}}{d\tau} + \frac{dI_{n+1,m}}{d\tau} \right) - L_y \left(\frac{dI_{n,m-1}}{d\tau} + \frac{dI_{n,m+1}}{d\tau} \right) = E(\tau), \\ I_{n,m} = \frac{dQ_{n,m}}{d\tau}, \end{array} \right. \quad (1)$$

where $I_{n,m}$ is the alternating current in the circuit with coordinates n and m , $Q_{n,m}$ is the charge, L and $L_{x,y}$ are the self-inductance and mutual inductance, R is the ohmic resistance, $E(\tau) = E_0 \sin \Omega \tau$ is the EMF induced by the alternating magnetic field $H(\tau) = H_0 \cos(\Omega \tau)$ so that $E_0 = \mu_0 \Omega S H_0$, where $\mu_0 = 4\pi \times 10^{-7}$ H/m is the magnetic permeability in vacuum, and S is the area of the split-ring resonator, $U_{n,m} = U(Q_{n,m})$ is the capacitive voltage nonlinearly depending on the magnitude of the charge.

In this paper, we consider the modification of a two-dimensional metamaterial consisting of nanoscale closely spaced rectangular resonators, which includes additional capacitive coupling between the resonators relative to model (1). It is shown in Fig. 1. It is generalized to the two-dimensional case of the one-dimensional model previously proposed by the authors of Ref. 16.

Capacitive coupling almost always exists between such resonators, and it has the same order of magnitude as inductive coupling.¹⁸ Local nonlinearity for each nanoelement in a metamaterial can be created by inserting a dielectric with Kerr nonlinearity into gaps of the split circuits, as shown in Fig. 1. The effect of nonlinearity is described by the cubic terms of the expansion in the dependence $U(Q_{n,m}) = Q_{n,m}(1 - \eta(Q_{n,m}/Q_c)^2)/C_0$, where C_0 is the linear capacitance of the split resonator as an oscillatory circuit, Q_c is the characteristic charge, and η is the numerical factor for the cubic

nonlinearity. For the generalized model [similarly to the first system Eq. (1)], we write the following equation for the voltage in the circuit with n and m coordinates, highlighting the second differences in the expressions for capacitive and inductive coupling and renormalizing the coefficients of induction and capacitance related to this node:

$$\begin{aligned} & \tilde{L} \frac{d^2 Q_{n,m}}{d\tau^2} + R \frac{dQ_{n,m}}{d\tau} + \tilde{C}^{-1} Q_{n,m} \\ & - \frac{\eta}{C_0 Q_c^2} Q_{n,m}^3 - C_x^{-1} (Q_{n-1,m} + Q_{n+1,m} - 2Q_{n,m}) \\ & - C_y^{-1} (Q_{n,m-1} + Q_{n,m+1} - 2Q_{n,m}) \\ & - L_x \frac{d^2}{d\tau^2} (Q_{n-1,m} + Q_{n+1,m} - 2Q_{n,m}) \\ & - L_y \frac{d^2}{d\tau^2} (Q_{n,m-1} + Q_{n,m+1} - 2Q_{n,m}) = E_0 \sin \Omega \tau. \end{aligned} \quad (2)$$

The renormalized coefficients have the following form: $\tilde{L} = L - 2(L_x + L_y)$ and $\tilde{C}^{-1} = C_0^{-1} - 2(C_x^{-1} + C_y^{-1})$, where C_x and C_y characterize the capacitive coupling between the resonators in the corresponding directions. It should be noted that Eq. (2) in its original form has eleven independent parameters.

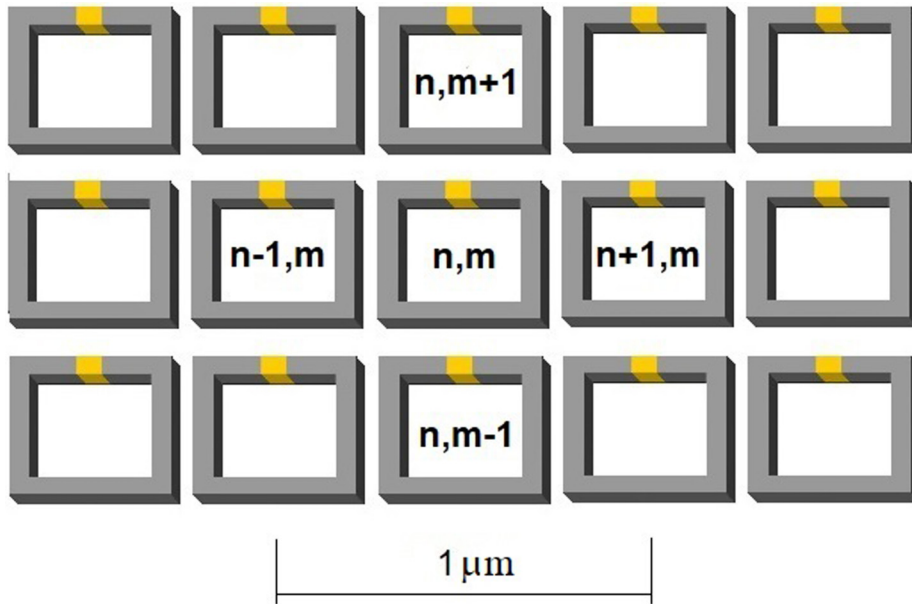


FIG. 1. Model of a two-dimensional terahertz metamaterial.

In the absence of EMF, the dispersion law for linear oscillations of this discrete model has the following form:

$$\Omega(k_x, k_y) = \Omega_0 \sqrt{\frac{1 + v_x^2 s^2(k_x) + v_y^2 s^2(k_y)}{1 + \lambda_x s^2(k_x) + \lambda_y s^2(k_y)}} \quad (3)$$

where the minimum frequency of self-oscillations in the metamaterial is as follows: $\Omega_0 = 1/\sqrt{\tilde{L}\tilde{C}}$; and parameters $\lambda_{x,y} = L_{x,y}/\tilde{L}$; $v_{x,y} = \Omega_{x,y}/\Omega_0 = \sqrt{\tilde{C}/C_{x,y}}$, $\Omega_{x,y} = 1/\sqrt{\tilde{L}C_{x,y}}$; $s(k_{x,y}) \equiv 2 \sin(\frac{1}{2}k_{x,y}d)$, d is the distance between the nanoresonators. Obviously, the spectrum (3) is bounded in frequency not only from below, but also from above.

It can be seen that in Eq. (2), the second time derivative of the second-order difference for the charge is a direct discrete implementation of the fourth mixed derivative. Therefore, in the long-wave limit, when the distance between the resonators (d) is much smaller than the oscillation wavelength, by complete analogy with the one-dimensional case¹⁶, Eq. (2) for the charge $Q_{n,m}$ directly reduces to the regularized two-dimensional nonlinear Klein-Gordon equation for the charge variable $u_{n,m} = Q_{n,m}/Q_c \rightarrow u(x, y, t)$, with additional terms describing the attenuation (ohmic resistance) and external variable force (EMF):

$$u_{tt} + \gamma u_t - u_{xx} - u_{yy} - \beta^x u_{xxtt} - \beta^y u_{yytt} + u - \sigma u^3 = e_0 \sin(\omega t). \quad (4)$$

The variable $u(x,y,t)$ depends on the dimensionless coordinates $x = nd/l_x$, $y = md/l_y$, and time $t = \Omega_0 \tau$; the subscripts in the function u denote the corresponding partial derivatives; the characteristic lengths are $l_{x,y} = v_{x,y}d \equiv d\sqrt{\tilde{C}/C_{x,y}} \gg d$, the oscillation

damping coefficient is $\gamma = R\tilde{C}/\tilde{L}$; parameters $\sigma = \eta\tilde{C}/C_0$, $\omega = \Omega/\Omega_0$ and $e_0 = E_0\tilde{C}/Q_c$ are the dimensionless pump frequency and amplitude. For the amplitude and dispersion parameters, we obtain the following expressions:

$$e_0 = \frac{\mu_0 H_0 \Omega S \tilde{C}}{Q_c} = \frac{\mu_0 S}{Q_c} \sqrt{\frac{\tilde{C}}{\tilde{L}}} \omega H_0, \quad (5)$$

$$\beta^{x,y} = \frac{L_{x,y} C_{x,y}}{\tilde{L}\tilde{C}} = \frac{L_{x,y}}{\tilde{L}} \left(\frac{d}{l_{x,y}}\right)^2.$$

Mixed derivatives, which naturally arise due to the inductive interaction between nanoresonators, take into account a higher dispersion contribution and significantly affect the linear excitation spectrum of Eq. (4) in the absence of external pumping, thereby making it bounded both from below and above. Its explicit form in dimensional variables obviously follows from Expression (3), where $s(k_{x,y})$ simply needs to be replaced by $k_{x,y}d$.

The dispersion parameters $\beta^{x,y}$ can have the same or opposite signs, determined by the signs of the inductances $L_{x,y}$, which depend on the mutual orientation of the neighboring resonators. For planar orientation, as shown in Fig. 1, they are positive, and the spectrum of the model in dimensionless variables is limited by the minimum frequency $\omega_0 = 1$ and the maximum frequency $\omega_{\max} \propto 1/\sqrt{\beta_{x,y}}$.

For axial orientation, when the axis passes through the centers of adjacent circuits, these parameters are negative. In the long-wave approximation, the dispersion parameters $\beta^{x,y}$ are small, and the width of the continuous spectrum area is large. However, due to the limited excitation spectrum in the regularized equation and the same spectrum property in the discrete model, the nonlinear dynamics in these systems can have the same features, as was

predicted and described by the theory of the crystal lattice.^{19,20} Therefore, the range of the dispersion parameters can be significantly expanded, and the results obtained by the regularized equation may be valid for the initial discrete model of the metamaterial.

It turns out that – despite the anisotropy of capacitive and inductive coupling, the large number of parameters, and the complexity of the long-wave Eq. (3) – the problem of forced localized breather oscillations in magnetic metamaterials at pump frequencies close to the lower edge of the spectrum can be significantly simplified and reduced to universal dependences.

FORCED BREATHER OSCILLATIONS IN A TWO-DIMENSIONAL MAGNETIC METAMATERIAL

Using a Kosevich–Kovalev asymptotic procedure^{16,17} in the non-dissipative case, i.e. assuming that Eq. (4) is solved in the form of a series of time harmonics at pump frequency and a small parameter of frequency splitting from the edge of the spectrum, $\kappa = \sqrt{1 - \omega^2} \ll 1$,

$$u(x, y, t) = A(x, y)\{[1 + \kappa^2 B(x, y)] \sin \omega t + \kappa^2 C(x, y) \sin 3\omega t + \dots\}, \quad (6)$$

we obtain the following nonlinear equation for the fundamental harmonic amplitude:

$$(1 - \beta^x \omega^2)A_{xx} + (1 - \beta^y \omega^2)A_{yy} - (1 - \omega^2)A + \frac{3}{4}\sigma A^3 + e_0 = 0. \quad (7)$$

After introducing new coordinates and renormalizing harmonic and force amplitudes,

$$X = \sqrt{\frac{1 - \omega^2}{1 - \beta^x \omega^2}}x, \quad Y = \sqrt{\frac{1 - \omega^2}{1 - \beta^y \omega^2}}y, \quad (8)$$

$$A = af \equiv \sqrt{\frac{4}{3\sigma}(1 - \omega^2)}f, \quad e_0 = \sqrt{\frac{4}{3\sigma}(1 - \omega^2)^{3/2}}p \quad (9)$$

we finally obtain the equation

$$\Delta f - f + f^3 + p = 0, \quad (10)$$

where Δ is the two-dimensional Laplacian in the new coordinates. This equation has three homogeneous solutions, the smallest of which determines a stable homogeneous background of oscillations far from the center of the system:

$$f_0 = \frac{1}{\sqrt{3}} \cos \frac{\gamma}{3} - \sin \frac{\gamma}{3}, \quad \gamma = \arccos \left(\frac{3\sqrt{3}}{2} p \right). \quad (11)$$

As can be seen, the parameter p can vary from zero to a maximum value of $p_c = 2/3^{3/2}$.

After the homogeneous background $f(X, Y) = f_0 + f_s(X, Y)$ is isolated from the solution, its soliton portion $f_s(X, Y)$ must satisfy

zero boundary conditions. We are interested in the radially symmetric solution to Eq. (10), which now reduces to the following:

$$\frac{d^2 f}{dr^2} + \frac{1}{r} \frac{df}{dr} - f + f^3 + p = 0, \quad (12)$$

where $r = \sqrt{X^2 + Y^2}$. At infinity, the function $f(r)$ reaches the constant value f_0 , and since the first derivative in Eq. (12) can be neglected in this limit, the asymptotic behavior of $f(r)$ coincides with the asymptotic behavior of the solution to the equation for the one-dimensional metamaterial as obtained in Ref. 16. When approaching zero, the solution reaches a constant value, having a zero derivative.

It is convenient to analyze possible soliton solutions, which satisfy the above boundary conditions, by interpreting Eq. (12) as the equation of motion of a particle in a nonlinear potential (Fig. 2).

If we omit the term with the first derivative and rewrite Eq. (12) as

$$\ddot{f} - f + f^3 + p = 0, \quad (13)$$

where the points mean differentiation by some effective time \tilde{t} , then it is easy to see that this equation of particle motion has the following energy integral E with the potential energy $U(f)$, as shown in Fig. 2:

$$E = \frac{1}{2} \dot{f}^2 + U(f), \quad U(f) = -\frac{1}{2} f^2 + \frac{1}{4} f^4 + pf. \quad (14)$$

Due to the integral of motion, both soliton solutions to Eq. (13) are explicit and describe the amplitudes of the fundamental harmonics of the only two possible breathers on a pedestal in a one-dimensional metamaterial.¹⁶ As can be seen in Fig. 2, the integral E is taken as equal to E_0 , in order to satisfy the necessary boundary conditions, i.e. when the amplitude reaches the constant value f_0 , or

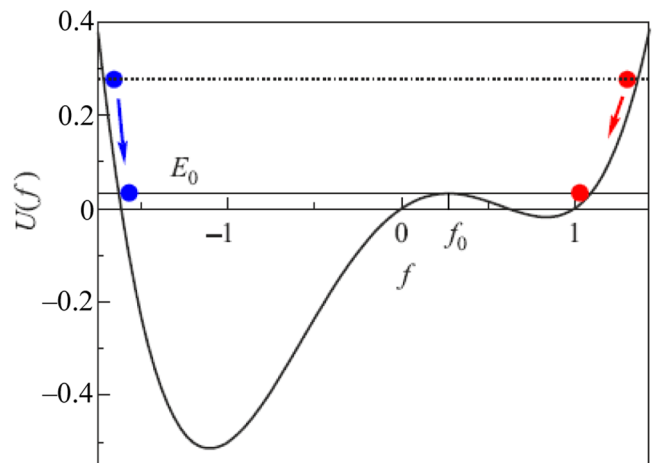


FIG. 2. Motion of a particle in a nonlinear potential.

to put it in terms of particle dynamics, when it infinitely approaches the local maximum of potential energy.

In the two-dimensional case, the need to take into account the first derivative in Eq. (12) is interpreted as the impact of effective friction on particle dynamics. When multiplied by the first derivative, this equation can be rewritten follows: $\dot{E} = -2F \equiv -\dot{f}^2/\dot{t}$. The positivity of the dissipative function F leads to a decrease in energy; therefore, the initial values of the particle energy are obviously chosen to be larger than E_0 values. It is easy to understand that there are, respectively, two sequences of positive and negative initial amplitudes, starting from which (at zero initial velocity) the coordinate of a particle will reach the constant asymptotic value f_0 . It follows from Fig. 2 that there are two main solutions whose amplitudes are completely located on one of the sides of the barrier. With a subsequent increase in the initial amplitude, the particle certainly overcomes the barrier and can reach a maximum with both a positive and a negative derivative. Thus, both sequences can be characterized according to this criterion. It should be noted that, when external force is absent and the potential is symmetric, the problem of the sequence of soliton states in the two-dimensional case was solved more than half a century ago.²¹ Within this limit, both sequences found in this study degenerate into one because the solutions in the symmetric case are determined up to a sign.

The results of the numerical integration of Eq. (12) with the above boundary conditions are shown in Figs. 3–5, where the parameter $p = 0.35$ is chosen close to p_c – the boundary of the existence of three homogeneous solutions. In a two-dimensional metamaterial, the main soliton modes on a pedestal are, similarly to the one-dimensional case,¹⁶ a completely positive solution (line 1, Fig. 3), or a “plus mode,” and a mode with the negative portion of the amplitude at the origin (line 2, Fig. 3), or a “minus mode.” It is the latter that corresponds to the oscillation in which the core region oscillates in antiphase to the homogeneous background and provides the local diamagnetic response of the metamaterial.

According to the earlier analysis, and in contrast to a one-dimensional metamaterial, a two-dimensional metamaterial has the main breathing modes along with more complex radially symmetric

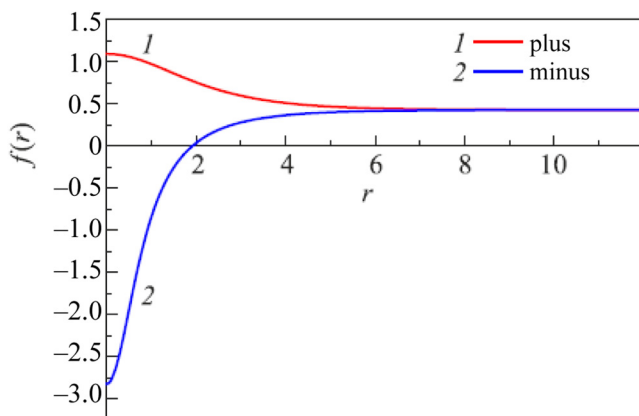


FIG. 3. Main oscillation modes of 2D solitons on a pedestal.

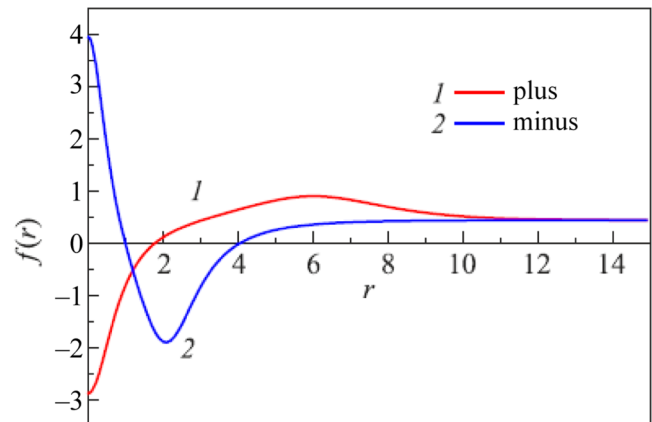


FIG. 4. First “excited” modes of 2D solitons.

solitons on a pedestal. Such solitons can be classified not only by the above criterion, but also by the number of zeros (Figs. 4 and 5); therefore, for convenience, they can be called “excited” oscillation modes.

It should be noted that with this choice of the parameter p , the minus-breather in Fig. 4 and the plus-breather in Fig. 5 turn out to be very close in shape but differ in the main criterion – the sign of the derivative at infinity.

LOCAL DIAMAGNETISM IN A TWO-DIMENSIONAL METAMATERIAL

Having a numerically determined solution for a two-dimensional dynamic soliton on a “pedestal” with a negative amplitude in the center, we can determine the magnetic permeability of a metamaterial containing such a breather excitation. This solution depends on only one parameter, p , and therefore it is universal enough to enable us to analyze various limiting cases of analytical

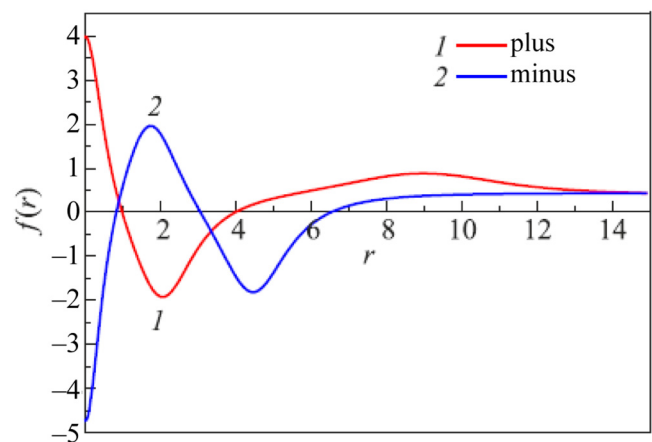


FIG. 5. Second “excited” modes of 2D solitons.

dependences when it comes to the dimensional characteristics of the metamaterial and pumping parameters. In particular, the solution remains equally valid for both isotropic and highly anisotropic capacitive and inductive coupling, as well as for the inductances L_x and L_y , which are opposite in sign and correspond to a metamaterial with the same axial orientation of split resonators.

Magnetic permeability is calculated in a standard way.^{9,16} The expression for magnetic induction is as follows:

$$B = \mu_0(H(\tau) + M(x, y, \tau)), \quad (15)$$

where $M(x, y, \tau)$ is the magnetization of the metamaterial at a point with coordinates (x, y) , which is determined by the current strength $I(x, y, \tau)$ in the circuit and is equal to $M(x, y, \tau) = Sd^{-3}\partial Q(x, y, \tau)/\partial\tau$. By substituting the solution $Q(x, y, \tau) = Q_c A(x, y) \sin \Omega\tau$ for induction, we obtain the following expression:

$$B = \mu_0\mu_r(x, y, \Omega)H_0 \cos \Omega\tau \quad (16)$$

with the relative permeability and magnetic susceptibility

$$\mu_r(x, y, \Omega) = 1 + \chi(x, y, \Omega), \quad (17)$$

$$\chi(x, y, \Omega) = \rho A(x, y, \Omega) = \rho a f(x, y, \Omega), \quad (18)$$

where the dimensionless parameter ρ and the estimate of the amplitude a have the form

$$\rho \equiv \frac{S\Omega}{H_0 d^3} Q_c, \quad a \approx \frac{\mu_0 H_0 \Omega S}{Q_c \tilde{L}(\Omega_0^2 - \Omega^2)}. \quad (19)$$

After estimating the area of the resonator by the formula $S \approx d^2$, we finally obtain the following expression:

$$\chi(x, y, \Omega) = \rho A(x, y, \Omega) \approx \frac{\Omega^2}{\Omega_0^2 - \Omega^2} \frac{\mu_0 d}{\tilde{L}} f(x, y, \Omega). \quad (20)$$

Magnetic terahertz metamaterials ($\Omega_0 \geq 10^{12}$ Hz) have the characteristic nanoscale dimensions of structural elements, as well as distances between them of the order of $d \approx 4 \times 10^{-7}$ m, and an inductance of $\tilde{L} \approx 10^{-12}$ H. Hence $\mu_0 d/\tilde{L} \approx 0.5$, and finally it turns out that $\rho a \gg 1$ due to the close proximity of Ω to Ω_0 . Thus, the sign of the magnetic permeability is completely determined by the dependence $A(x, y, \Omega)$, and the diamagnetic response in the breather localization region substantially exceeds the positive response of the homogeneous background (Fig. 6).

Figure 6 shows a soliton contribution to magnetization oscillations, which are locally antiphase with respect to the homogeneous background in the center of the two-dimensional metamaterial. The evolution of a breather on a pedestal has been calculated for a system which measures 300×300 , is composed of resonant circuits with $\beta_{x,y} = 0.25$, and is located in the field of a terahertz electromagnetic wave with a frequency of $\Omega = 0.997 \Omega_0$, a period of $T_\Omega = 2\pi/\Omega$, and a pump amplitude characterized by the dimensionless parameter $p = 0.25$. Two breather profiles are given for the time after

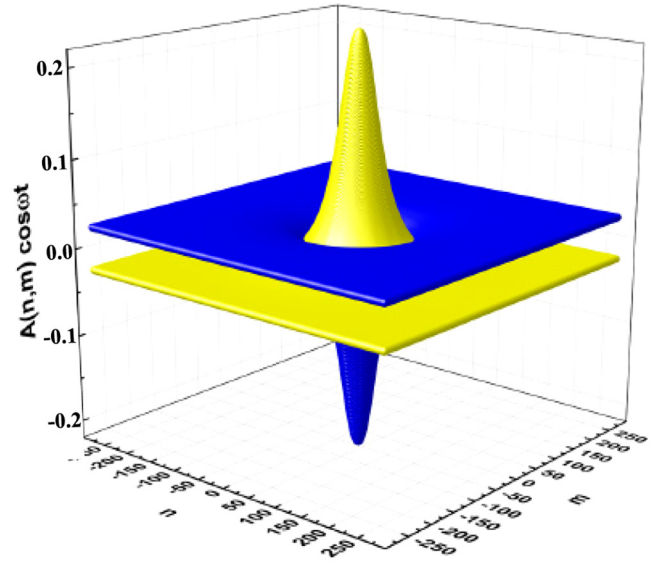


FIG. 6. Contribution of a breather on a pedestal to magnetization oscillations, which demonstrate regions with positive and negative permeability, i.e. nonlinear diamagnetic response in the center of the lattice of split rectangular resonators.

150 periods of oscillations with an interval of half a period. During the entire oscillation time, the breather remained virtually unchanged, and its amplitude did not actually differ from the initial profile, which was chosen as an analytically obtained solution. As can be seen in the figure, there are up to a hundred of resonators in the central region of the negative magnetic permeability, which is indeed a macroscopic characteristic of the magnetic metamaterial.

METASTABILITY OF TWO-DIMENSIONAL BREATHERS AND SCENARIOS FOR THE DEVELOPMENT OF THEIR INSTABILITY

The lifetime of the detected breather excitations plays an important role in observing the effect of local diamagnetism in two-dimensional metamaterials. The obtained approximate solutions to the regularized nonlinear Klein–Gordon equation describe stationary oscillations. At the same time, it is known that in two-dimensional nonlinear equations with only the second spatial derivatives, particularly in a two-dimensional sine-Gordon equation, breathers are not stable,²² and the search for their stabilization parameters is a separate problem.²³ In some magnetic models,²⁴ the inclusion of higher spatial derivatives can stabilize solitons because strong dispersion can compensate for nonlinearity in such equations and prevent the collapse of localized states. Therefore, inductive coupling in a metamaterial, which generates the fourth mixed derivatives, should be fully taken into account even at small dispersion values. On the other hand, it should be noted that if these values are not small, then the spectral area of linear oscillations will be narrow. Then the frequency of the third harmonic of a soliton on a pedestal will be above the area, which guarantees the absence of

direct excitation of linear waves by a breather and its loss of energy through radiation. It follows from the above that the stability of two-dimensional breathers under pumping conditions depends on many factors and almost all parameters of the original problem.

It follows from the results simulating the dynamics of a breather on a pedestal (as obtained as part of the discrete integration scheme, and as shown in Fig. 6) that there exists a range of values that are quite permissible in the developed theory, where long-lived forced oscillations bring about local negative magnetic permeability and the diamagnetic response of a two-dimensional metamaterial. At the same time, since the regularized Eq. (4) with pumping is not integrable, it should be expected that its soliton solutions are metastable. To solve this problem by numerical simulation, we studied the evolution of radially symmetric breathers on a pedestal, in the framework of Eq. (4) in dependence on the dispersion parameters $\beta_{x,y} = \beta$, and the amplitude and frequency of pumping. The fundamental harmonic of the solution (6) and its time derivative with amplitudes satisfying Eq. (12) were taken as the initial condition. The difference between the exact and approximate solutions served as the initial perturbation, the evolution of which made it possible to examine the stability of the exact solution. Due to the radial symmetry of the solutions, it is radially symmetric exponentially increasing components that are the source of instability of such solitons. This fact is also confirmed by the integration of the original equation on a square lattice (Fig. 6), as a result of which the solution always maintains a radially symmetric shape. This enables us to study the evolution of breathers within the framework of the “radial” regularized nonlinear Klein–Gordon equation with periodic external force:

$$u_{tt} - \Delta_r(u + \beta u_{tt}) + u - \sigma u^3 = e_0 \sin(\omega t), \quad (21)$$

where Δ_r is the radial part of the two-dimensional Laplacian.

The numerical calculation confirmed that the closer the frequency ω to the uniform resonance frequency ω_0 , the longer the breather lifetime and the closer the analytical expression for the fundamental harmonic to the exact solution. With an increase in the breather amplitude, the time of the onset of instability rapidly decreases, therefore, the main calculations were performed for a frequency of $\omega = 0.997$ and, accordingly, for an oscillation period of $T = 2\pi / \omega \cong 6.302$.

The results of a numerical simulation of the dynamics of breathers are presented in Figs. 7–13. Figure 7(a) shows the profiles of a minus-breather on a pedestal of homogeneous oscillations as radial equation solutions after 150 periods of oscillations. In fact, they reproduce a breather solution on a square lattice (Fig. 6). However, in the same figure, which shows the radial dependence of the breather profiles in one oscillation period at an interval of 1/8 of a period, we can see how an instability mode manifests itself. According to Fig. 7(a), at the very moment when the solution proportional to $\sin(\omega t)$ should vanish, there is a small non-zero component proportional to $\cos(\omega t)$, which, along with a small component proportional to $\sin(\omega t)$, forms a radially symmetric instability mode. The amplitude of this instability mode grows exponentially with a rather small increment. In the time series of oscillations of the breather amplitude at the origin in Fig. 7(b), we can see the beginning of this growth. Although in general, the breather remains visually almost unchanged and, as can be seen, has a long lifetime.

Over the course of further evolution, the instability mode grows, and the breather itself grows in amplitude [Fig. 8(a)], and as can be seen in the time series [Fig. 8(b)], it finally loses stability after a transition period with a decrease in amplitude, which is accompanied by an infinite increase in amplitude, i.e. by collapse. Further investigation of the dependence of the instability development on the value of the dispersion parameter explains this result.

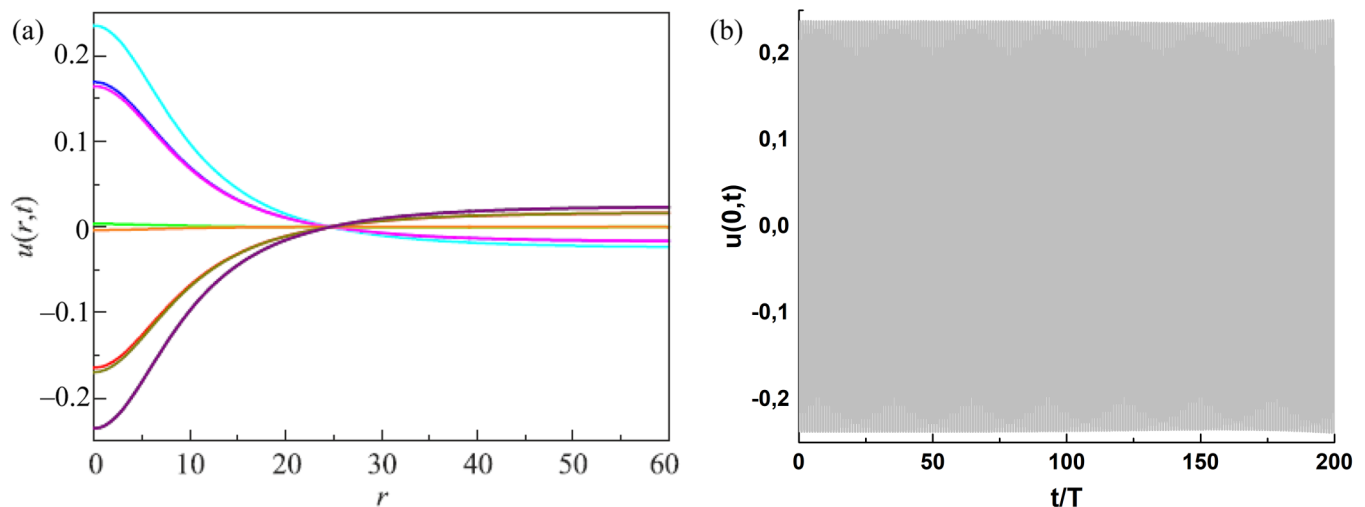


FIG. 7. (a) Profiles of a minus-breather after 1/8 of a period after $t = 150T$ and (b) time series of oscillations of the amplitude of this breather at the origin. ($\beta = 0.25$ and $\rho = 0.25$).

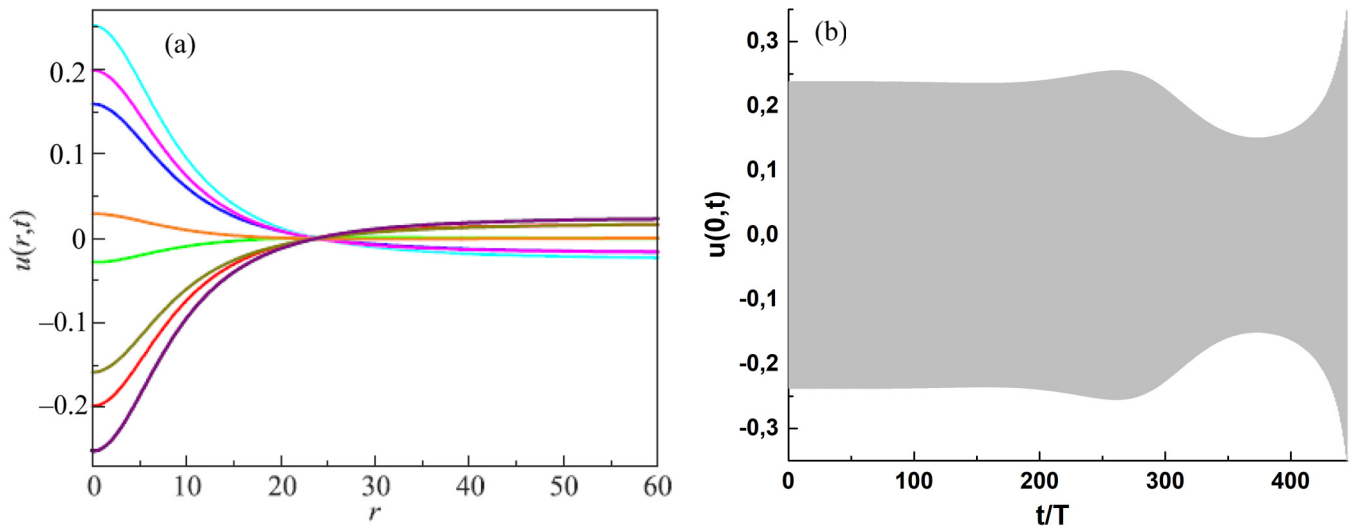


FIG. 8. (a) Profiles of a minus-breather with an instability mode after $t = 250T$ and (b) time series of oscillations of the amplitude of this breather at the origin. ($\beta = 0.25$ and $p = 0.25$).

At very small values of the dispersion parameter β , when mixed derivatives can be neglected, the regularized equation tends to the limit of the conventional nonlinear Klein–Gordon equation, in which, as is known, the instability of a two-dimensional breather terminates in collapse.²² This is exactly what is seen in Fig. 9(a), which shows the time dependence of the amplitude in the center of a soliton at $\beta = 0.0075$.

However, at large β , taking into account higher dispersion leads to a fundamental change in the scenario for instability

development [Fig. 9(b)]. In this case, the change in the breather amplitude initially follows a collapse scenario, but ends with a sharp drop in the amplitude of the transformed breather and its further decay into radial waves.

The same transition between the scenarios is observed with respect to the pumping parameter p at the fixed dispersion parameter β (Fig. 10). It can be seen that at a pumping value close to the limiting value, the lifetime of a metastable minus-breather decreases substantially, and it actually transforms into a plus-

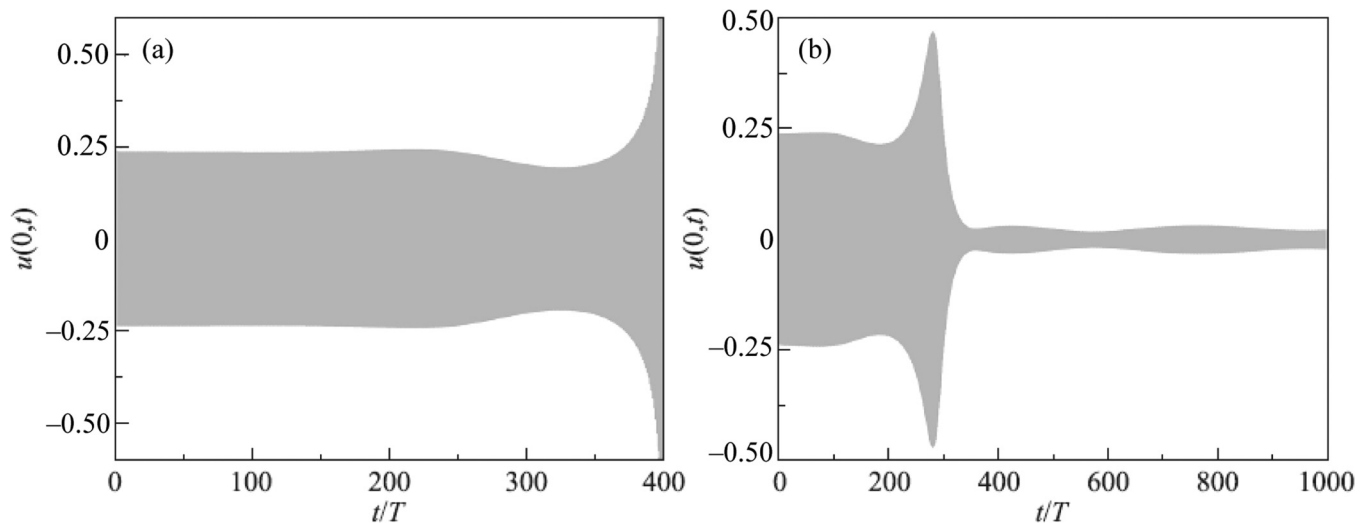


FIG. 9. (a) Time series for the amplitude of a minus-breather at very small β values ($\beta = 0.0075$) and (b) at large β values ($\beta = 0.75$). (Parameter $p = 0.25$).

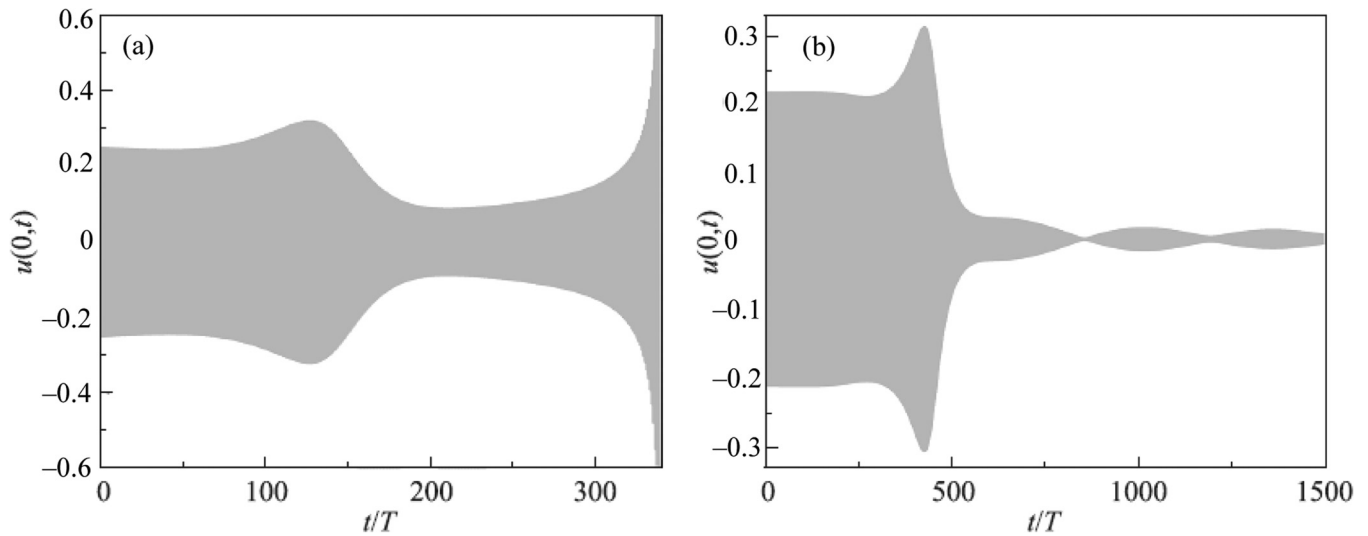


FIG. 10. Time series for the amplitude of a minus-breather at (a) $\rho = 0.35$ and (b) $\rho = 0.1$. (Fixed parameter $\beta = 0.25$).

breather, which eventually collapses [Fig. 10(a)]. The instability at low pump values results in the decay of the breather into radial waves [Fig. 10(b)].

It should be noted that the transformation of the minus-breather into the plus-breather, as the pump amplitude approaches the maximum possible value, and the subsequent stabilization of the plus-breather, are explained by the fact that within this limit it degenerates into a homogeneous nonlinear oscillation. As the pump amplitude decreases from its limiting value, the effect of the minus-breather transformation into the

plus-breather continues up to the boundary between the scenarios, which is subject to both the p parameter and the β parameter. At this boundary, the development of plus-breather instability leads to the occurrence of chaotic oscillation regimes, which ultimately end in collapse (Figs. 11 and 12). The occurrence of chaos is not unexpected because it becomes possible even in one nonlinear oscillator given considerable pumping.²⁵ Fig. 11(a) shows a time series of the evolution of a breather at $\beta = 0.47$ and $p = 0.25$. It follows therefrom that a metastable minus-breather with a long lifetime loses stability and transforms into a long-lived

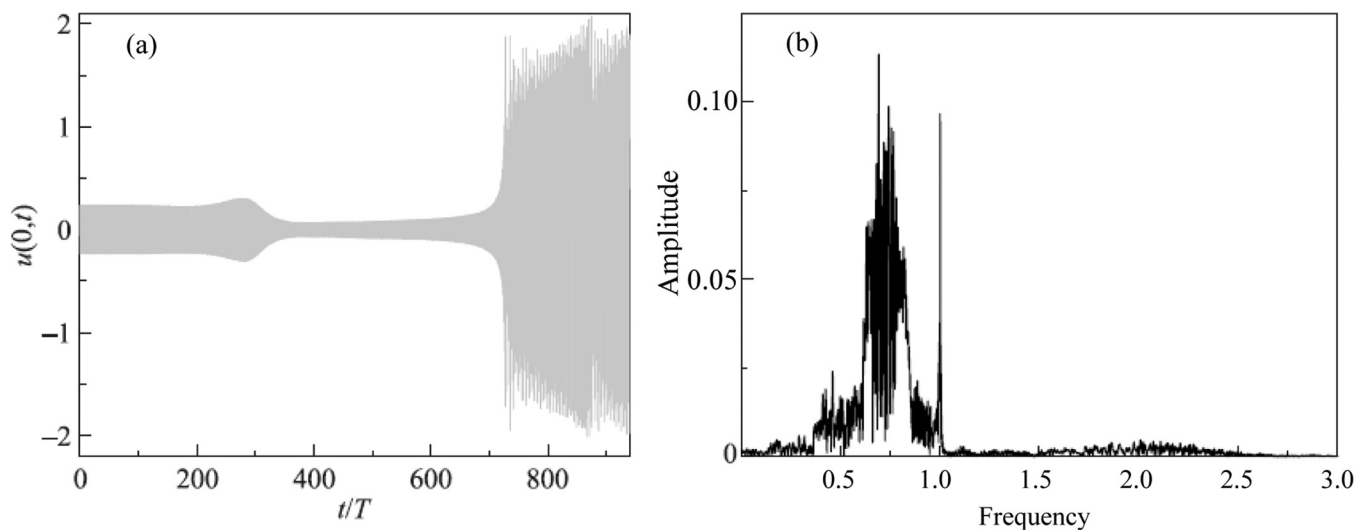


FIG. 11. (a) Time series for breather amplitude at $\beta = 0.47$ and $\rho = 0.25$, and (b) its chaotic frequency spectrum.

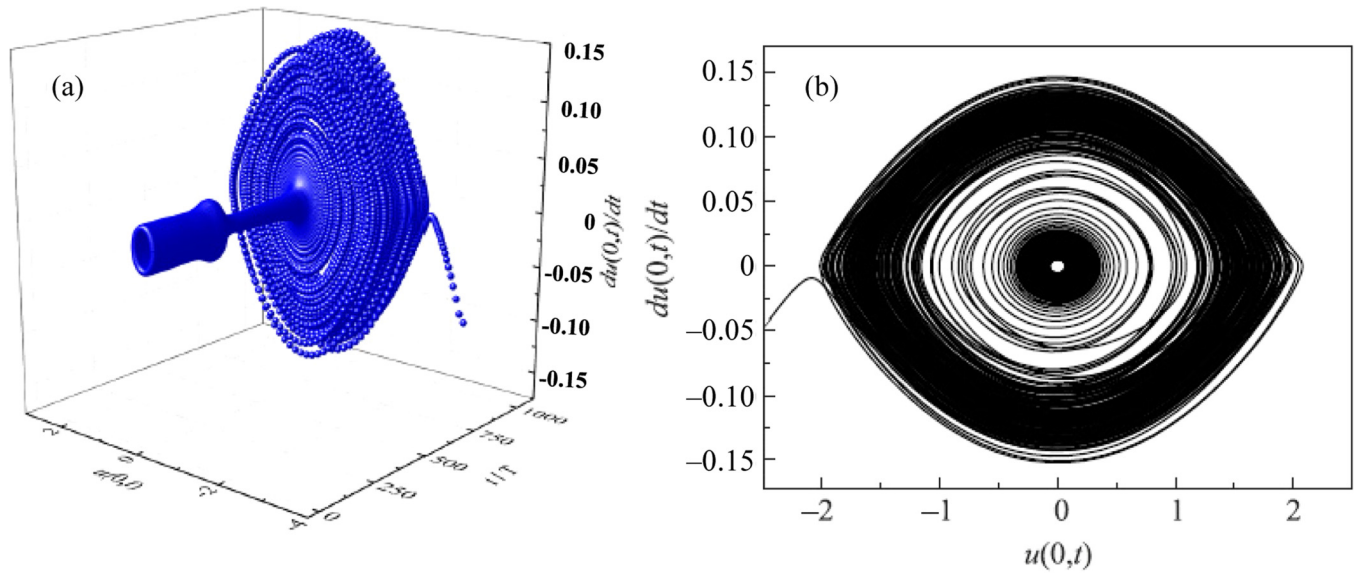


FIG. 12. (a) Evolution of an amplitude- phase portrait at the origin for $\beta = 0.47$ and $\rho = 0.25$, and (b) its frontal projection.

plus-breather, which, after loss of stability, turns into a large-amplitude breather with a chaotic spectrum of oscillations [Fig. 11(b)].

Figure 12(a) shows a time evolution of the phase portrait of the amplitude in the center of a breather, and Fig. 12(b) shows a frontal projection of the portrait. As can be seen, the plus-breather and the minus-breather correspond to almost stable cycles, and the large breather corresponds to the phase trajectories characteristic of

the stochastic layer near the separatrix for a nonlinear oscillator with Hamiltonian chaos.²⁵

Figure 13(a) shows completely spatially coherent profiles of a large breather after 850 oscillation periods, and Fig. 13(b) shows the stochastic waves it generates, on an enlarged scale. The leading edge of the regular waves is generated by a metastable minus-breather, and these waves continue to move after many oscillation periods following its disappearance.

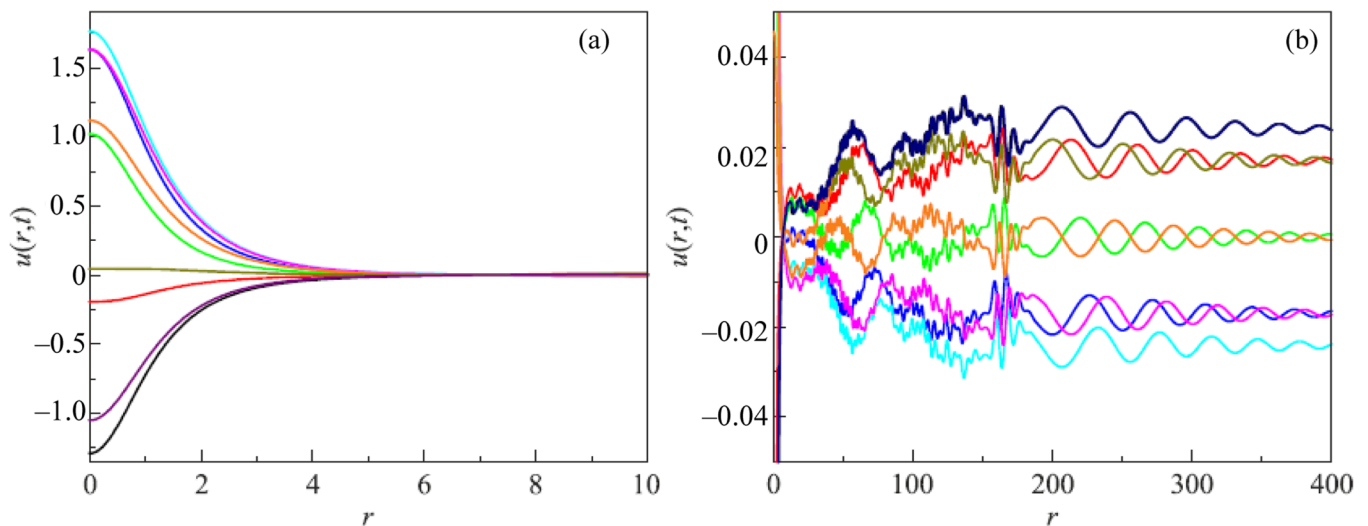


FIG. 13. (a) Profiles of a large-amplitude breather after 850 oscillation periods, and (b) chaotic oscillations generated thereby. ($\beta = 0.47$, $\rho = 0.25$).

Chaotic oscillations in Fig. 13 border on a spatially coherent localized nonlinear excitation, i.e. a breather and regular waves, thus exemplifying a chimera state in the dynamics of a two-dimensional nonlinear metamaterial.²⁶

Finally, it should be noted that as their structure becomes more complex, the remaining breathers on a pedestal (“excited” modes) have a shorter lifetime compared to the fundamental breather mode, which has a sufficiently long lifetime of up to hundreds of oscillation periods to manifest itself in an experiment on the detection of diamagnetic response of the metamaterial to an electromagnetic field in the terahertz range.

CONCLUSION

The main findings and conclusions of this study are as follows:

1. We have analytically and numerically investigated the nonlinear magnetic excitations in a two-dimensional system of nanoscale resonators with inductive and capacitive coupling, when applying an electromagnetic field in the terahertz range. It has been shown that in the long-wave limit, the dynamic equations for a variable charge that describe this system are reduced to the regularized two-dimensional nonlinear Klein–Gordon equation with the mixed fourth derivatives, which has an additional pump term as an external force.

2. An asymptotic method has been used to obtain radially symmetric breather-like solutions to such an equation. A two-dimensional nonlinear equation has been derived for the amplitude of the fundamental harmonic, and we have obtained two sequences of dynamic solitons on a pedestal – two-dimensional breathers that exist against the background of homogeneous oscillations. One of them has a large negative amplitude in the central region with a positive background amplitude, which corresponds to the local diamagnetic response of the metamaterial to an electromagnetic field and provides it with local negative magnetic susceptibility and permeability.

3. We have numerically studied the stability of breather-like fundamental modes as a function of the dispersion parameters (magnitude of inductive coupling), frequency, and pump amplitude. It has been established that all the nonlinear excitations obtained are metastable, but their lifetime can reach up to hundreds of oscillation periods. A negative amplitude breather is the most long-lived; and if its frequency is close to the lower boundary of the continuous spectrum, its lifetime can reach several hundred oscillation periods.

4. We have investigated the further evolution of a two-dimensional metastable breather, and have established two scenarios for the development of its instability, depending on the parameters of dispersion and pump amplitude. If the dispersion parameter is less than critical, the breather ultimately exhibits a collapse-like behavior after a small increase and then decrease in its amplitude. If the dispersion parameter is higher than the critical value, the breather finally splits into divergent regular waves after a short interval of amplitude growth. At the critical value of the dispersion parameter, a long-lived large-amplitude breather suddenly turns into a long-lived breather with a small positive amplitude, which then also rapidly turns into a chimera state that has a spatially

coherent large-amplitude breather that generates stochastic waves diverging from it.

Thus, it has been shown that in two-dimensional magnetic metamaterials affected by a terahertz electromagnetic field, the excitation of long-lived breather oscillations may give rise to a diamagnetic response that corresponds to local negative magnetic permeability. The theory of this effect has been developed for metamaterials with both isotropic and anisotropic inductive and capacitive coupling between split rectangular resonators forming a two-dimensional metamaterial.

The described effect makes it possible to observe two-dimensional magnetic breather excitations. If a two-dimensional system of split nanoscale resonators is supplemented, for example, with a lattice of conducting nanoelements that has a negative permittivity in the terahertz frequency range, then the refractive index will be negative in the magnetic breather localization region, and purely imaginary everywhere outside this region. As a result, the metamaterial region with an excited breather is transparent for the passage of an electromagnetic wave and can be detected experimentally. It should be noted that the established possibility of a soliton-type dependence in the spatial distribution of negative magnetic permeability by the proposed metamaterial model brings the idea of metamaterial cloaking closer to practical realization, which requires spatially dependent negative refractive indices.

ACKNOWLEDGMENTS

This work has been done using grid/cluster computing facilities at the B. I. Verkin Institute for Low Temperature Physics and Engineering, National Academy of Sciences of Ukraine, Kharkiv.

REFERENCES

- ¹V. G. Veselago, *Physics-Uspeski* **92**, 517 (1967).
- ²J. B. Pendry, A. J. Holden, D. J. Robbins, and W. J. Stewart, *IEEE Trans. Microwave Theory Tech.* **47**, 2075 (1999).
- ³D. R. Smith, W. Padilla, D. Vier, S. C. Nemat-Nasser, and S. Schultz, *Phys. Rev. Lett.* **84**, 4184 (2000).
- ⁴S. A. Ramakrishna and T. M. Grzegorzczuk, *Physics and Applications of Negative Refractive Index Materials* (SPIE Press & CRC Taylor & Francis Group, Boca Raton London New York, 2009).
- ⁵T. J. Yen, W. J. Padilla, N. Fang, D. C. Vier, D. R. Smith, J. B. Pendry, D. N. Basov, and X. Zhang, *Science* **303**, 1494 (2004).
- ⁶S. Linden, C. Enkrich, M. Wegener, J. Zhou, T. Koschny, and C. M. Soukoulis, *Science* **306**, 1351 (2004).
- ⁷C. M. Soukoulis, *Optics Photonics News* **17**, 16 (2006).
- ⁸N. Lazarides, M. Eleftheriou, and G. P. Tsironis, *Phys. Rev. Lett.* **97**, 157406 (2006).
- ⁹M. Eleftheriou, N. Lazarides, and G. P. Tsironis, *Phys. Rev. E* **77**, 036608 (2008).
- ¹⁰M. Lapine, I. V. Shadrivov, and Y. S. Kivshar, *Rev. Mod. Phys.* **86**, 1093 (2014).
- ¹¹N. Lazarides and G. P. Tsironis, *Appl. Phys. Lett.* **90**, 163501 (2007).
- ¹²O. V. Charkina and M. M. Bogdan, *Fiz. Nizk. Temp.* **44**, 824 (2018) [*Low Temp. Phys.* **44**, 644 (2018)].
- ¹³M. M. Bogdan, V. I. Belan, and O. V. Charkina, *Fiz. Nizk. Temp.* **44**, 1700 (2018) [*Low Temp. Phys.* **44**, 1331 (2018)].
- ¹⁴A. Pimenov, A. Loidl, P. Przyślupski, and B. Dabrowski, *Phys. Rev. Lett.* **95**, 247009 (2005).

- ¹⁵N. N. Rosanov, N. V. Vysotina, A. N. Shatsev, I. V. Shadrivov, and Y. S. Kivshar, *JETP Lett.* **93**, 743 (2011).
- ¹⁶M. M. Bogdan and O. V. Charkina, *Fiz. Nizk. Temp.* **40**, 303 (2014) [*Low Temp. Phys.* **40**, 234 (2014)].
- ¹⁷M. M. Bogdan and O. V. Charkina, *Fiz. Nizk. Temp.* **34**, 713 (2008) [*Low Temp. Phys.* **34**, 564 (2008)].
- ¹⁸P. Gay-Balmaz and O. J. F. Martin, *J. Appl. Phys.* **92**, 2929 (2002).
- ¹⁹P. Rosenau, *Phys. Rev. B* **36**, 5868 (1987).
- ²⁰M. M. Bogdan, A. M. Kosevich, and G. A. Maugin, *Wave Motion* **34**, 1 (2001).
- ²¹R. Y. Chiao, E. Garmire, and C. H. Townes, *Phys. Rev. Lett.* **13**, 479 (1964).
- ²²V. G. Makhankov, *Phys. Rep.* **35**, 1 (1978).
- ²³B. Piette and W. J. Zakrzewski, *Nonlinearity* **11**, 1103 (1998).
- ²⁴A. M. Kosevich, B. A. Ivanov, and A. S. Kovalev, *Nonlinear Magnetisation Waves. Dynamic and Topological Solitons* (Naukova Dumka, Kiev, 1983).
- ²⁵Y. I. Neimark and P. S. Landa, *Stochastic and Chaotic Fluctuations* (Nauka, Moscow, 1987).
- ²⁶Y. Kuramoto and D. Battogtokh, *Nonlinear Phenom. Complex Syst.* **5**, 380 (2002).

Translated by [AIP Author Services](#)